

Assessing the aggregation behaviour of iron oxide nanoparticles by using a multi-method approach.

Laura Chekli^a, Sherub Phuntsho^a, Jaya Kandasamy^a and Hokyong Shon^{a*}

^aSchool of Civil and Environmental Engineering, University of Technology, Sydney (UTS), Post Box 129, Broadway, NSW 2007, Australia.

*Corresponding author: Email: Hokyong.Shon-1@uts.edu.au

ABSTRACT

Iron nanoparticles are becoming increasingly popular for the treatment of contaminated soil and groundwater; however, their mobility and reactivity in subsurface environments are significantly affected by their tendency to aggregate. Assessing their stability under environmental conditions is crucial for determining their environmental fate. A multi-method approach (including different size-measurement techniques) was used to thoroughly characterise the behaviour of iron oxide nanoparticles (Fe₂O₃NPs) under environmentally relevant conditions. Although recent studies have demonstrated the importance of using a multi-method approach when characterising nanoparticles, the majority of current studies continue to use a single-method approach.

Discussions and examples to support the need of a multi-method approach to characterise the aggregation of nanoparticles will be presented in this study.

Keywords: Iron oxide nanoparticles, aggregation, multi-method approach.

1 INTRODUCTION

In the past few years, a variety of iron oxide nanoparticles have been investigated for environmental remediation purposes. Despite the potential efficacy of these materials, many laboratory and pilot-scale field studies have demonstrated that the mobility and reactivity of iron-based nanoparticles are substantially limited in natural porous systems (e.g. soils and groundwater aquifers) [1-4]. Aggregation is considered to be the primary cause of reduced mobility and reactivity, and this phenomenon is the result of many factors including solution pH, ionic strength and the presence of organic matter [5, 6]. In the case of iron-based nanoparticles, previous studies have investigated that these nanoparticles have pH-dependant surface charges and that extensive aggregation due to charge neutralisation occurs near the point of zero charge (PZC) [7-10]. Furthermore, soil and groundwater conditions are often characterised by high ionic strength and high concentrations of monovalent (e.g., Na⁺, K⁺) and divalent (e.g., Ca²⁺, Mg²⁺) cations in the mM range; factors that are known to

reduce electrostatic repulsion between particles and thereby enhance aggregation [11].

In this study, characterisation of bare Fe₂O₃NPs and the aggregation behaviour of these nanoparticles under relevant environmental conditions (i.e. pH, particle concentration and ionic strength) were performed using flow field-flow fractionation (FIFFF), dynamic light scattering (DLS) and scanning electron microscopy (SEM). Although the characterisation of manufactured nanoparticles (MNPs) can be considerably simpler than it is for natural particle samples, MNPs are also complex, and a multiple characterisation approach is necessary to ensure the accuracy of the characterisation data [12, 13]. In fact, due to analytical challenges, the lack of appropriate characterisation data in environmentally realistic conditions is a major limitation of current research in this area. As such, there is clearly a need for useful characterisation tools that can assist in assessing MNP behaviour under relevant environmental conditions. Flow field-flow fractionation (FIFFF) is well suited to measuring MNP behaviour under relevant conditions simply by modifying the mobile phase used during characterisation. However, one of the main limitations of FIFFF is related to material losses during analysis. These generally occur via particle-membrane interaction and adsorption and may represent up to 50% of the injected mass [14].

This is the first time that FIFFF has been applied to study the aggregation behaviour of Fe₂O₃NPs under relevant environmental conditions. The results have been compared with those from other size-measurement techniques to provide increased confidence in the outcomes.

2 MATERIALS AND METHODS

2.1 FIFFF analysis

The FIFFF used in our experiment is an asymmetrical AF2000 Focus (Postnova Analytics, Germany) with channel length of 29.8 cm (tip to tip), channel width of 2 cm and channel thickness of 0.025 cm. The detection system comprises a UV/Vis detector operating at a 254 nm wavelength (SPD 20A from Shimadzu, Japan). The software AF2000 Control, version 1.1.0.23 (Postnova Analytics) is used to control the FIFFF system. A

regenerated cellulose membrane (Z-AF4-MEM-612-10KD, Postnova Analytics, Germany) with a molecular weight cut-off of 10 kDa is used as a channel wall. Sodium azide (0.1 mM NH_3) is systematically used in the mobile phase for all experiments to prevent bacteria growth. The sample volumes are all 20.8 μL and are injected using 50 μL sample loop (Rheodyne Corporation, CA, USA). Latex beads of 22 nm, 58 nm, 100 nm and 410 nm are used to create calibration curves from which hydrodynamic diameters of the particles were determined. These curves correlate the retention time to particle size.

2.2 DLS analysis

A Zetasizer (model ZEN3600; Malvern Instruments, Worcestershire, UK) operating with a He-Ne laser at a wavelength of 633 nm is used to determine the zeta potential and hydrodynamic diameter of the different samples.

2.3 SEM analysis

Silicon wafers attached on carbon stubs are used for SEM measurements. About 10 μL of sample is deposited on a silicon wafer and left to dry completely. Images are obtained from a Zeiss Supra 55VP variable pressure SEM (Carl Zeiss AG, Germany) and recorded using SmartSEM® software. The mean equivalent circular diameter is determined from these images.

3 RESULTS AND DISCUSSIONS

3.1 Effect of particle concentration

Size measurements by DLS were performed at different particle concentrations ranging from 10 to 200 mg/L, and different pH values from pH 2 to 12 (Figure 1). It should be noted that samples with particles with Z-average hydrodynamic diameter > 1,000 nm (i.e. 1 μm) were settling during the analysis; however, DLS can only be used when particles are strictly subjected to Brownian motion. Thus, these data are only indicative of the agglomeration trend and cannot be used as accurate or absolute measurements.

At all particle concentrations, maximum aggregation was reached at the PZC where the net particle surface charge was reduced to zero, as shown in Figure 1. Far from this point, particle aggregate sizes decrease because particles are stabilised by electrostatic repulsion forces.

The results also show a particle size concentration dependence at nanoparticle concentrations above 50 mg/L, especially at $\text{pH} > 5$. This is presumably due to the fact that when particle concentration increases, the distance between the particles in the sample is reduced, which increases the chance of collision between particles and hence, their aggregation. Previous studies (Baalousha 2009; Dickson et al. 2012) indicated similar findings for this concentration range. It should be noted here that injected concentrations

of $\text{Fe}_2\text{O}_3\text{NPs}$ on contaminated sites are generally between 1 to 10 g/L (Saleh et al. 2008), and aggregation phenomena are expected to be even more exacerbated in this high concentration range.

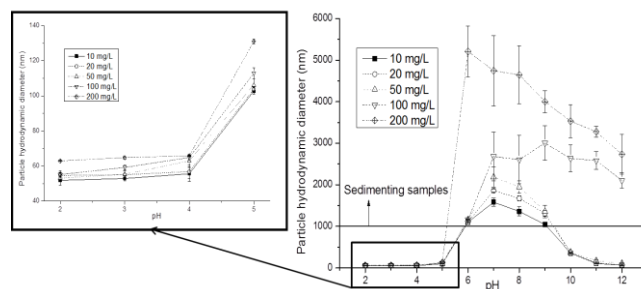


Figure 1: Influence of particle concentration on the Z-average hydrodynamic diameter of $\text{Fe}_2\text{O}_3\text{NPs}$ at different pH, as measured by DLS.

3.2 Effect of pH

The effect of pH on the aggregate size of $\text{Fe}_2\text{O}_3\text{NPs}$ at a concentration of 50 mg/L has been investigated by FIFFF, DLS and SEM (Table 1). The size analysis showed a good agreement among the three measurement techniques. In general, the sizes measured by SEM were comparable to FIFFF sizes, while the sizes measured by DLS were generally larger than FIFFF as shown in Table 1. DLS is known to be very sensitive to larger particles and a very small number of large particles (e.g. formed during the aggregation process) can induce a substantial shift toward larger sizes [13].

Table 1: Summary of the hydrodynamic diameter of $\text{Fe}_2\text{O}_3\text{NPs}$ at variable pH as determined from FIFFF/UV, DLS and SEM at 50 mg/L.

pH	FIFFF results (nm)	DLS results (nm)	SEM results (nm)
3	27.1±0.2	55.3±2.4	25±2
4	41.4±0.1	63.0±3.9	35±4
5	80.3±0.8	106.1±3.6	80±7
7	Samples could not be analysed by FIFFF and DLS due to sedimentation of the particles prior to the analysis		1500±137
10	132.1±5.8	377.5±3.6	250±32

However, at pH 10, a significant difference in size was observed using the SEM, FIFFF and DLS techniques; the FIFFF derived sizes in particular, were much lower than those from other techniques showing the limitation of this technique. This could be explained by the fact that, at this pH, both the FFF membrane and $\text{Fe}_2\text{O}_3\text{NPs}$ are negatively charged. Thus, in addition to the concentration gradient

effect that drives the diffusion of particles back into the channel, electrostatic repulsive forces also arise between particles and the membrane, causing lower retention times than expected and translating into an underestimation of particle size.

3.3 Effect of ionic strength

Figure 2 shows the FIFFF/UV fractograms of Fe₂O₃NPs as a function of ionic strength, and Table 2 gives the corresponding hydrodynamic diameters obtained from the FFF fractograms as well as the Z-average hydrodynamic diameters obtained by DLS measurements.

The DLS results show an increase in particle aggregate sizes with increasing ionic strength. At low ionic strength (1 mM-5 mM NaCl and 0.5 mM CaCl₂), the Z-average hydrodynamic diameter varies slightly from 63.19 to 64.92 nm. This is not significantly different from the size of nanoparticles measured in ultrapure water. This indicates that at low ionic strength, electrostatic repulsive forces are dominant over the attractive forces, preventing particles from aggregating. However, the use of 10 mM NaCl or 2 mM CaCl₂ resulted in particle aggregation, probably due to the reduction in repulsive forces between particles.

The FIFFF fractograms (Figure 2) show no change in the retention times with increased ionic strength but a significant decrease in the UV signal intensity is observed. The constant elution time is expected as it has been demonstrated in previous studies that ionic strength has no effect on retention time of particles of the same size [15, 16]. Dubascoux et al. [15] explained that an increase in ionic strength leads to a decrease in the double layer thickness of particles, which promotes the formation of larger aggregates. These larger clusters of particles will be located closer to the FFF membrane which will increase the collisions between the membrane and these larger aggregates. Thus, they could be irreversibly adsorbed onto the membrane which would explain the observed decrease in the UV signal.

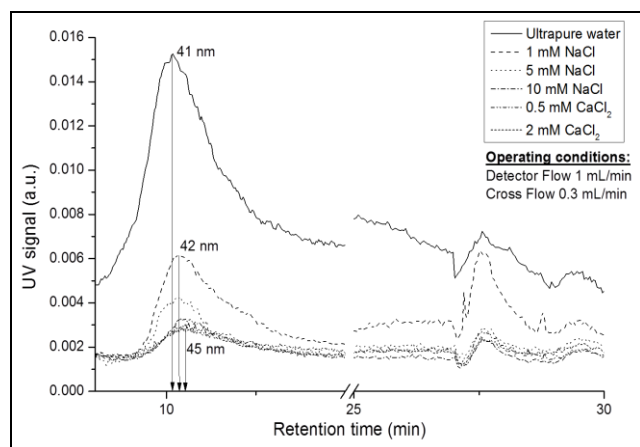


Figure 2: FIFFF fractograms of Fe₂O₃NPs (50 mg/L; pH 4) at variable ionic strength.

Table 2: Hydrodynamic diameter (FFF) and Z-average hydrodynamic diameter (DLS) of Fe₂O₃NPs as a function of ionic strength.

Ionic strength	Particle size (nm)	
	FIFFF/UV	DLS
Ultrapure water	41.4 ± 0.1	61.4 ± 1.4
1 mM NaCl	42.3 ± 0.1	63.2 ± 3.6
5 mM NaCl	42.8 ± 1.7	64.4 ± 5.2
10 mM NaCl	44.7 ± 2.5	312.4 ± 10.7
0.5 mM CaCl ₂	44.4 ± 0.6	64.9 ± 4.9
2 mM CaCl ₂	44.8 ± 2.7	438.7 ± 18.1

4 CONCLUSION

The stability of Fe₂O₃NPs has been investigated under different environmental conditions by using several analytical techniques. The need for a multi-method approach is critical because every method has its own limitations. For instance, one of the limitations of DLS is the polydispersity of the sample which leads to an over-estimation of the average particle size. With FFF, one of the limitations arises from the interaction between the membrane and the particles which can jeopardise the results if some of the larger particles are adsorbed onto the membrane; furthermore the pH dependent changes in the surface charge of the NPs, which controls the interaction with membrane, may limit the suitability of latex beads as references for particle size. Therefore, the use of FFF with mobile phases mimicking environmentally relevant conditions may not provide definitive answers in terms of particle size as in this case most measurements will not be made using an optimised mode of operation. The presence of large aggregates (i.e. above 1 µm) and sedimentation of these aggregates during the analysis were also a significant limitation to the collection of accurate and reliable data. Therefore, this study shows that it is essential to deploy a number of analytical and theoretical techniques to investigate the behaviour of NPs. Other analytical methods that can measure the size of aggregates in this size range with greater accuracy (e.g. low-angle laser light scattering (LALLS) techniques) should also be considered.

REFERENCES

1. Schrick, B., et al., *Delivery vehicles for zerovalent metal nanoparticles in soil and groundwater*. Chemistry of Materials, 2004. **16**(11): p. 2187-2193.
2. Saleh, N., et al., *Surface modifications enhance nanoiron transport and NAPL targeting in saturated porous media*. Environmental Engineering Science, 2007. **24**(1): p. 45-57.
3. Quinn, J., et al., *Field demonstration of DNAPL dehalogenation using emulsified zero-valent iron*. Environmental Science and Technology, 2005. **39**(5): p. 1309-1318.
4. He, F. and D. Zhao, *Manipulating the size and dispersibility of zerovalent iron nanoparticles by use of carboxymethyl cellulose stabilizers*. Environmental Science and Technology, 2007. **41**(17): p. 6216-6221.
5. Ponder, S.M., J.G. Darab, and T.E. Mallouk, *Remediation of Cr(VI) and Pb(II) aqueous solutions using supported, nanoscale zero-valent iron*. Environmental Science and Technology, 2000. **34**(12): p. 2564-2569.
6. Saleh, N., et al., *Adsorbed triblock copolymers deliver reactive iron nanoparticles to the oil/water interface*. Nano letters, 2005. **5**(12): p. 2489-2494.
7. Baalousha, M., *Aggregation and disaggregation of iron oxide nanoparticles: Influence of particle concentration, pH and natural organic matter*. Science of the Total Environment, 2009. **407**(6): p. 2093-2101.
8. Baalousha, M., et al., *Aggregation and surface properties of iron oxide nanoparticles: Influence of pH and natural organic matter*. Environmental Toxicology and Chemistry, 2008. **27**(9): p. 1875-1882.
9. Hu, J.-D., et al., *Effect of dissolved organic matter on the stability of magnetite nanoparticles under different pH and ionic strength conditions*. Science of the Total Environment, 2010. **408**(16): p. 3477-3489.
10. Sun, Y.-P., et al., *Characterization of zero-valent iron nanoparticles*. Advances in Colloid and Interface Science, 2006. **120**(1-3): p. 47-56.
11. Saleh, N., et al., *Ionic strength and composition affect the mobility of surface-modified FeO nanoparticles in water-saturated sand columns*. Environmental Science & Technology, 2008. **42**(9): p. 3349-3355.
12. Lead, J.R. and K.J. Wilkinson, *Aquatic colloids and nanoparticles: current knowledge and future trends*. Environmental Chemistry, 2006. **3**(3): p. 159-171.
13. Domingos, R.F., et al., *Characterizing manufactured nanoparticles in the environment: multimethod determination of particle sizes*. Environmental science & technology, 2009. **43**(19): p. 7277-7284.
14. Hassellöv, M. and R. Kaegi, *Environmental and Human Health Effects of Nanoparticles*, ed. J.R. Lead and E. Smith 2009, Chichester: Wiley.
15. Dubascoux, S., et al., *Optimisation of asymmetrical flow field flow fractionation for environmental nanoparticles separation*. Journal of Chromatography A, 2008. **1206**(2): p. 160-165.
16. Shon, H.K., et al., *A study on the influence of ionic strength on the elution behaviour of membrane organic foulant using advanced separation tools*. Desalination and Water Treatment, 2009. **11**(1-3): p. 38-45.